

# Coexistence in the two-dimensional May–Leonard model with random rates

Qian He<sup>1</sup>, Mauro Mobilia<sup>2</sup>, and Uwe C. Täuber<sup>1</sup>

<sup>1</sup> Department of Physics, Virginia Tech, Blacksburg, Virginia 24061-0435, U.S.A.  
e-mail: heq07@vt.edu; tauber@vt.edu

<sup>2</sup> Department of Applied Mathematics, School of Mathematics, University of Leeds, Leeds LS2 9JT, U.K.  
e-mail: M.Mobilia@leeds.ac.uk

Received: June 14, 2011/ Revised version: date

**Abstract.** We employ Monte Carlo simulations to numerically study the temporal evolution and transient oscillations of the population densities, the associated frequency power spectra, and the spatial correlation functions in the (quasi-)steady state in two-dimensional stochastic May–Leonard models of mobile individuals, allowing for particle exchanges with nearest-neighbors and hopping onto empty sites. We therefore consider a class of four-state three-species cyclic predator-prey models whose total particle number is not conserved. We demonstrate that quenched disorder in either the reaction or in the mobility rates hardly impacts the dynamical evolution, the emergence and structure of spiral patterns, or the mean extinction time in this system. We also show that direct particle pair exchange processes promote the formation of regular spiral structures. Moreover, upon increasing the rates of mobility, we observe a remarkable change in the extinction properties in the May–Leonard system (for small system sizes): (1) As the mobility rate exceeds a threshold that separates a species coexistence (quasi-)steady state from an absorbing state, the mean extinction time as function of system size  $N$  crosses over from a functional form  $\sim e^{cN}/N$  (where  $c$  is a constant) to a linear dependence; (2) the measured histogram of extinction times displays a corresponding crossover from an (approximately) exponential to a Gaussian distribution. The latter results are found to hold true also when the mobility rates are randomly distributed.

**PACS.** XX.XX.XX No PACS code given

## 1 Introduction

The rock–paper–scissors (RPS) system [1, 2, 3, 4, 5] or, equivalently, three-species cyclic predator-prey models, have been widely studied in order to understand biodiversity in ecology and biology [6, 7, 8, 9, 10]. As a non-trivial model for cyclic competition [11], RPS as well as its variants constitute paradigmatic model systems to mathematically describe the co-evolutionary dynamics of three coexisting species in cyclic competition, such as, e.g., realized in nature for three types of Californian lizards [12, 13], and the coexistence of three strains of *E. coli* bacteria in microbial experiments [14]. Among the various RPS variants, a particular model introduced by May and Leonard [5] has recently received much attention [15, 16, 17, 18, 19], leading to novel results that have important implications for the formation and propagation of spatial patterns in ecological systems.

It has been demonstrated that in non-spatial model systems with RPS-type competition, two of the three species typically evolve towards extinction in finite observable time [18, 20, 21]. However, when spatial degrees of freedom and species dispersal and associated interactions between nearest-

neighbor particles are allowed, e.g., in lattice-based Monte Carlo simulations, the spatial fluctuations and correlations induce a coexistence state of all three species, and the emergence of intriguing spatio-temporal structures [11, 15, 16, 17, 19, 22, 23, 24, 25, 26, 27]. In particular, the authors of Refs. [15, 16, 17] studied a stochastic two-dimensional version of the four-state RPS game (May–Leonard model) where the conservation law for the total population density is removed, and found that mobility (particle pair exchange together with hopping) has a critical influence on species diversity. Significantly, when the mobility exceeds a well-defined threshold, the typical size of spiral patterns outgrows the system size, and eventually species coexistence in the system is destroyed [15, 19].

Coexistence and competition of biological species are often crucially affected by environmental influences which include limited and randomly distributed natural resources, the availability of shelter, varying climate conditions, etc. Therefore, it is important to understand the precise role of spatial inhomogeneity on the formation and development of biodiversity. In previous work concerned with a four-state RPS system with conserved total particle number [28], we have found that spatially varying reaction rates

have little effect on the dynamical evolution. In this paper, our goal is to numerically study the effect of spatial disorder on species coexistence in two-dimensional stochastic May–Leonard model variants. To this end, we implement the reaction (and mobility) rates for the May–Leonard dynamics as quenched random variables that for each lattice site are independently drawn from a truncated Gaussian distribution, and subsequently held fixed during the simulation run. We here explore (i) the self-organization of the population in the coexistence phase, (ii) compute the spatio-temporal correlation functions, and (iii) investigate the statistics of species extinction times (for small system sizes). Our main results can be summarized as follows:

(1) We demonstrate that quenched spatial disorder has only minor effect on species coexistence in the May–Leonard model, which together with the results reported in Ref. [28], shows that RPS models (in the presence or absence of total particle number conservation) form a class of systems that are robust against environmental variability. Remarkably, this statement is true even when spatial disorder affects the particles’ mobility which is known to drastically impact species coexistence.

(2) We study the combined effect of pair exchange and hopping processes, and demonstrate that the former are more important for the formation of robust spiral wave structures.

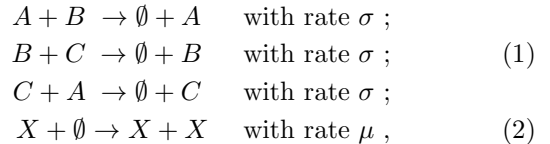
(3) We compute the extinction times, defined as the time when the first one of three species dies out, in (small) spatially extended systems. We thus find that the mean extinction time (MET) increases sharply with system size  $N$  when the mobility rate is low and the system is in the (long-lived metastable) coexistence state. However, once the mobility exceeds the threshold beyond which species extinction is prevalent, the MET function switches to a linear dependence on  $N$ . Correspondingly, the extinction time distribution is found to cross over from approximately exponential with prominent tail at large times, to a bell-shaped near-Gaussian function.

This paper is structured as follows: In Sec. 2, we define the stochastic spatial May–Leonard model as a four-state spatial rock–paper–scissors (RPS) game without conservation law for the total particle number, and briefly discuss the well-established results from the mean-field rate approximation approach. In Sec. 3, we first explain how this stochastic spatial system is implemented in our Monte Carlo simulations on a two-dimensional lattice, and introduce the quantities of interest. Then we present and analyze our simulation results. Finally, in Sec. 4 we conclude with a discussion and interpretation of our findings.

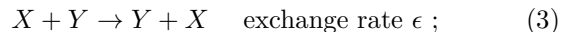
## 2 Model and rate equations

In the mean-field approximation, our spatial system reduces to the original May–Leonard model<sup>1</sup> [5]. We let all populations live on a square lattice, with each lattice site

occupied with at most a single individual. We therefore allow four states per site: three interacting particle species that we label  $A$ ,  $B$ , and  $C$ , and an empty state  $\emptyset$ . The model is defined through the following set of binary predation and offspring production reactions between the three particle species [5, 15, 16]:



where  $X \in (A, B, C)$  refers to any one of the three species. Note that in contrast with the conventional rock–paper–scissors model [18, 20, 28, 29, 30, 31], the total particle number is *not* conserved by these reactions, owing to the separation of predation and reproduction processes. In addition, in our spatially-extended system we consider the nearest-neighbor particle exchange and hopping processes on a two-dimensional square lattice (with periodic boundary conditions; here again  $X, Y = A, B, C$ ):



It is worth mentioning that the models studied in Refs. [15, 16, 17] do not separate the hopping process (4) from pair exchange (3); i.e.,  $\epsilon = D$ . Therefore, when letting  $\epsilon = D$  and in the absence of any quenched disorder, our spatial model coincides with the one investigated in Refs. [15, 16, 17].

May and Leonard [5] studied the associated deterministic mean-field rate equations and obtained the temporal evolution of the population densities. Let  $a(t)$ ,  $b(t)$ , and  $c(t)$  represent the population densities (concentrations) of species  $A$ ,  $B$ , and  $C$ , respectively. Since at most one individual is allowed on each site in the simulation, within the mean-field approximation, the overall population density  $\rho(t) = a(t) + b(t) + c(t)$  restricts the reproduction processes (2). Therefore, the corresponding rate equations are

$$\begin{aligned} \partial_t a(t) &= a(t) [\mu (1 - \rho(t)) - \sigma c(t)] , \\ \partial_t b(t) &= b(t) [\mu (1 - \rho(t)) - \sigma a(t)] , \\ \partial_t c(t) &= c(t) [\mu (1 - \rho(t)) - \sigma b(t)] . \end{aligned} \quad (5)$$

The coupled rate equations (5) yield four linearly unstable absorbing states  $(a, b, c) = (0, 0, 0)$ ,  $(1, 0, 0)$ ,  $(0, 1, 0)$ , and  $(0, 0, 1)$ , and one reactive fixed point  $(a^*, b^*, c^*) = \frac{\rho^*}{3}(1, 1, 1)$ , where  $\rho^* = \frac{3\mu}{3\mu + \sigma}$ , representing coexistence between the three species. Linearizing around the coexistence fixed point leads to

$$\begin{pmatrix} \partial_t \delta a \\ \partial_t \delta b \\ \partial_t \delta c \end{pmatrix} = L \begin{pmatrix} \delta a \\ \delta b \\ \delta c \end{pmatrix} , \quad (6)$$

where  $\delta a(t) = a(t) - a^*$ ,  $\delta b(t) = b(t) - b^*$ , and  $\delta c(t) = c(t) - c^*$ , and with the linear stability matrix  $L$

$$L = \frac{-\mu}{3\mu + \sigma} \begin{pmatrix} \mu & \mu & \mu + \sigma \\ \mu + \sigma & \mu & \mu \\ \mu & \mu + \sigma & \mu \end{pmatrix} . \quad (7)$$

<sup>1</sup> At the mean-field level, the model considered here corresponds to the original May–Leonard model [5] with parameters  $\alpha = 1$  and  $\beta = 1 + \sigma/\mu$ , and time measured in units of  $1/\mu$ .

Its eigenvalues are  $\lambda_1 = -\mu$ , and  $\lambda_{2,3} = \frac{\mu\sigma}{2(3\mu+\sigma)}[1 \pm \sqrt{3}i]$ , which demonstrates that the fixed point is locally stable only in one direction of parameter space (the eigenvector associated with the negative eigenvalue  $\lambda_1$ ), and generally linearly unstable. As elaborated in Refs. [15,16,17], the system dynamics quickly approaches an invariant manifold associated with the rate equations (5). In the neighborhood of the unstable interior fixed point  $(a^*, b^*, c^*)$ , the invariant manifold is tangent to the plane normal to the eigenvector of  $L$  associated with  $\lambda_1$  [17]. On this invariant manifold, the trajectories approach the absorbing boundaries of the phase portrait where they linger and form a heteroclinic cycle [2,5]. In this case, any chance fluctuations can cause species extinction by deviating the trajectories toward the absorbing boundaries. From the imaginary part of the complex conjugate eigenvalues  $\lambda_{2,3}$ , we infer the characteristic oscillation frequency  $\omega = \sigma\rho^*/2\sqrt{3}$ .

### 3 Monte Carlo simulation results for the spatially-extended May–Leonard model

We investigate the two-dimensional May–Leonard model, i.e., the four-state stochastic RPS game defined by the reactions (1,2) (which do not conserve the total particle number) on a two-dimensional lattice (typically with  $N = 256 \times 256$  sites) with periodic boundary conditions, subject to the nearest-neighbor exchange (3) and hopping (4) processes. In order to mimic finite local carrying capacities, we impose a maximum occupancy number of one particle (of either species) per lattice site. When investigating the effect of spatial disorder on the model, we will treat one of the rates ( $\mu, \sigma, \epsilon$ , or  $D$ ) at each lattice site as a random number drawn from a normalized Gaussian distribution truncated at one standard deviation on both sides. For example,  $\mu \sim N(m, n)$  implies that the rate  $\mu$  is picked from a truncated normal distribution on the interval  $[m - n, m + n]$ , centered at the value  $m$  with standard deviation  $n < m$ . In practice, a value of  $\mu$  is drawn from  $N(m, n)$  for each site on the lattice and attached to the corresponding site at the beginning of each single Monte Carlo run. The rate values remain unchanged for all sites until the next run is initiated. Therefore, in our model, the randomized rates pertain to the lattice sites; but are identical for any individual landing on a given site for each single run.

At each simulation step, an individual of any species on the lattice is selected randomly; then one of its four nearest-neighbor sites, which might be empty or occupied by one particle of either three species, is selected at random. Subsequently, the particles undergo the pair reaction (1), reproduction (2), exchange (3), or hopping (4) processes, according to the respective associated rates. Once on average each of the  $P$  individual particles on the lattice has had a chance to react, reproduce, exchange, or move, one Monte Carlo step (MCS) is completed; the infinitesimal simulation time step is thus  $\delta t \sim P^{-1}$ .

When studying the effect of quenched spatial disorder in the reaction and mobility rates, we shall focus on inves-

tigating a base model with (average) mobility rate set to 5, since the corresponding pure system displays clearly established spiral waves (see Fig. 1b below). Whenever neither fixed rate values nor their distribution are specified below, the following default rate values were implemented in the simulations:  $\mu = \sigma = 1$ , and  $\epsilon = D = 5$ . We shall characterize the emerging spatial structures through instantaneous snapshots of the particle distribution in the lattice, and will depict the temporal evolution of population (spatially averaged) densities. Because of the underlying symmetry among the species  $A$ ,  $B$ , and  $C$ , one representative population suffices and we here report results for the spatial average of local population number  $n_A(j, t)$  of species  $A$ , i.e., the spatially averaged density  $a(t) = \langle n_A(j, t) \rangle = \frac{1}{N} \sum_j n_A(j, t)$ , where  $j$  represents the site index. We shall also obtain the associated Fourier transform

$$a(f) = \int a(t) e^{2\pi i f t} dt, \quad (8)$$

and compute the equal-time two-point correlation functions in the (quasi-)steady state,

$$C_{AB}(x, t) = \langle n_A(j+x, t) n_B(j, t) \rangle - a(t) b(t), \quad (9)$$

where  $j$  denotes the site index, and similarly for  $C_{AA}(x, t)$ , etc. For our typical system size of  $N = 256 \times 256$  sites we never observed the extinction state in our simulations. In fact, as discussed in Ref. [15] and below (see Sec. 3.3), in this case one expects the extinction time to grow exponentially with the system size. Therefore, in order to access absorbing states and numerically measure the mean extinction time (MET)  $\bar{T}_{\text{ex}} = \langle T_{\text{ex}} \rangle$ , where  $T_{\text{ex}}$  is the extinction time for a single Monte Carlo run, and extract extinction time distributions, we must consider small systems of sizes  $N = 25$  to 225.

#### 3.1 Self-organization in the three-species coexistence phase

In the first row of Fig. 1, we plot typical snapshots of the spatial particle distributions at  $t = 1000$  MCS for various exchange and diffusion rates, as indicated, while  $\mu = \sigma = 1$  are held fixed. We observe in Fig. 1a that all three species coexist and a set of entangled spiral patterns forms in the system when the mobility rates are comparatively low. Upon increasing the mobility rates, the spiral patterns expand, see Fig. 1b. When the spirals' typical size  $\ell$  at last outgrows the lattice for large particle mobility (compare Fig. 1a–1c), we anticipate that the system essentially acquires the features of its zero-dimensional stochastic counterpart (see Sec. 3.3 and Ref. [15]). In that situation, the system evolves towards one of the three absorbing states wherein two species become extinct, and the surviving species uniformly fills the lattice (uniform phase). In finite systems therefore, there exists a threshold set by the condition  $\ell \approx L = \sqrt{N}$  (in a square lattice) that separates the absorbing states from species coexistence. Since the typical extent of the spirals grow diffusively as  $\ell \sim \sqrt{2\epsilon}, \sqrt{2D}$ , this transition should occur

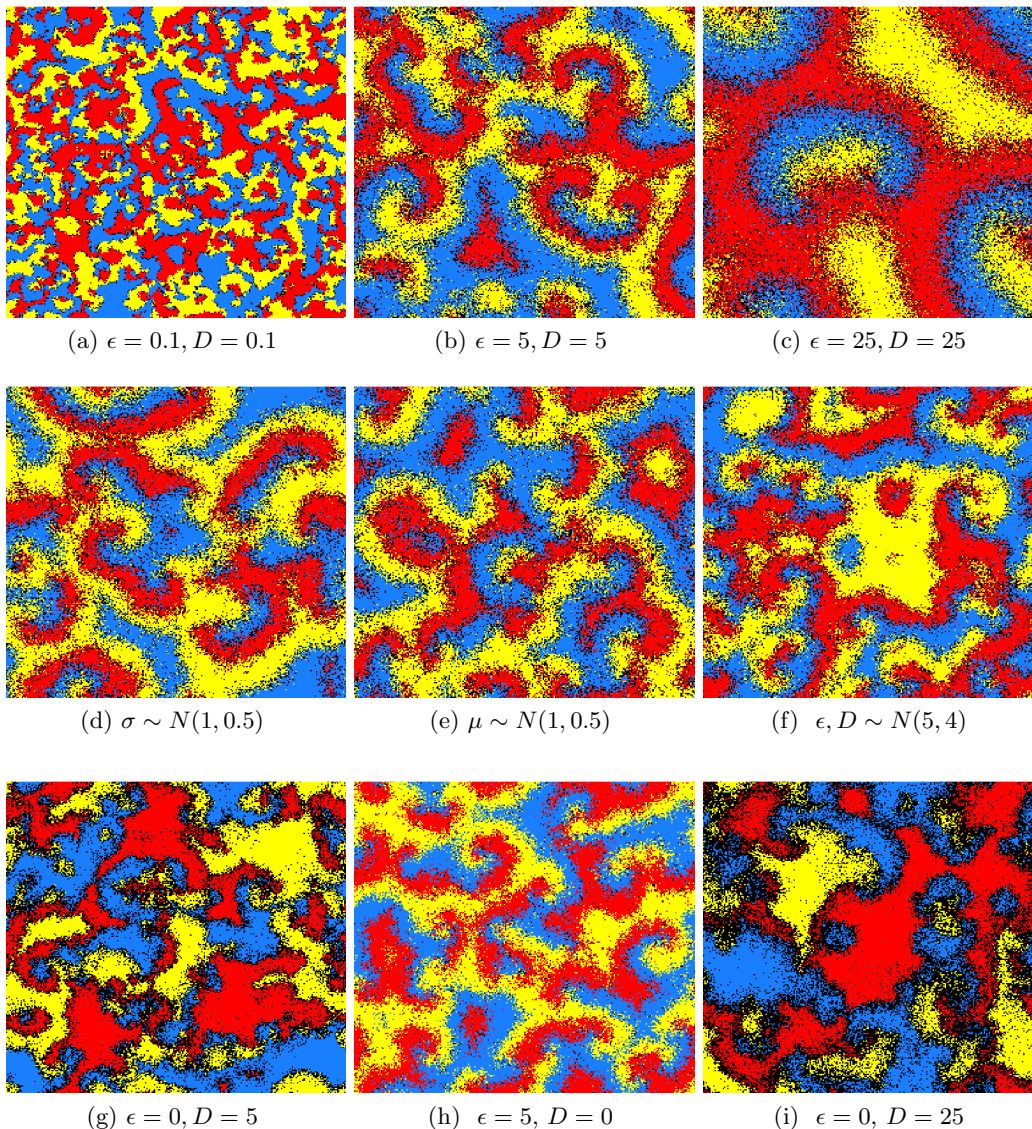


Fig. 1: (*Color online.*) Snapshots of the spatial particle distribution at  $t = 1000$  MCS for a system with  $N = 256 \times 256$  sites with equal initial densities  $a(0) = b(0) = c(0) = 1/3$ . If not specified otherwise, the corresponding default rate values are implemented  $\mu = \sigma = 1$ ,  $\epsilon = D = 5$ . (red/gray:  $A$ , yellow/light gray:  $B$ , blue/dark gray:  $C$ , black: empty).

at some critical value  $M_c$  of the scaled effective mobility  $M = 2(\epsilon, D)/N$  [15].

In two-species predator-prey systems, quenched spatial disorder in the reaction rates can markedly enhance both asymptotic particle densities in two-species predator-prey systems [32]; yet this finding is not corroborated in three-species RPS models with conserved total population [28]. Thus we next explore the effect of spatial variability in the reaction as well as in the mobility rates in the spatial stochastic May–Leonard model where the conservation law for the total particle number has been removed, and where the mean-field dynamics is *not* characterized by neutrally stable orbits [2, 5, 18, 20]. To this end, we introduce quenched spatial disorder by treating the rate on

each site of the lattice as a random variable drawn from a truncated Gaussian distribution. As shown in the snapshots in the second row of Fig. 1 (compare with Fig. 1b), the presence of spatial clustering can still be observed even though small noisy spiral structures dominate the system. Thus, the spatial disorder does not markedly affect the formation and occurrence of spiral patterns.

The third row of Fig. 1 shows snapshots of the system after removing either the two-particle exchange process (3) or pure nearest-neighbor hopping (4). When exchange processes are not allowed, see Figs. 1g and 1i, cluster formation is still observed, while the spiral waves become rather noisy, and it is worth noticing that one additional cluster type consisting of only empty sites appears in the

system (discernible as black patches in Figs. 1g and 1i), with measurable consequences on physical observables, as will be discussed below. Moreover, in Fig. 1h where only exchange processes are allowed, the spiral pattern boundaries appear quite distinctly sharp, while the empty sites are randomly distributed rather than clustered.

From these results, we infer that the formation of the observed spiral patterns is promoted by pair exchange processes. Furthermore, we have also verified that the above scenario is not affected when the rates are randomly distributed and therefore remains robust against spatial variability of the reaction rates.

### 3.2 Time evolution and spatio-temporal correlation functions

In order to quantitatively characterize the properties of the system, the influence of quenched spatial disorder, and the effect of pure particle pair exchange processes on the evolution of system, we next depict the temporal evolution of population density  $a(t) = \langle n_A(j, t) \rangle$ , the associated Fourier transforms  $a(f)$ , and the spatial auto- and cross-correlation functions  $C_{AA}$  and  $C_{AB}$ , respectively, in the quasi-stationary state (here, at time 1000 MCS) in Fig. 2. Since the reaction processes are symmetric with respect to the three species, the quantities associated with species  $A$  suffice to extract the relevant information for all three species. As shown in Fig. 2a, the population density decreases swiftly at the beginning of the simulation runs: as the particles are initially randomly distributed and fill the entire lattice, predation reactions (1) dominate and deplete the particle density at the beginning. However, with the emergence of spiral patterns, these reactions can only take place along the domain boundaries of distinct species. The system then evolves towards the (quasi)-steady state with population densities  $\approx 0.26$  for the set of rates chosen here, consistent with the mean-field prediction  $a^* = \frac{\mu}{3\mu + \sigma} = 0.25$ .

In Fig. 2b, we depict the amplitude of the Fourier signal of the population density. The peak in  $|a(f)|$  yields a characteristic oscillation frequency  $\approx 0.004$ . This is almost a factor ten smaller than the prediction from the mean-field approximation,  $f = \omega/2\pi = \sqrt{3}/16\pi \approx 0.034$ , indicating a strong downward renormalization as consequence of spatial fluctuations and correlations, similar to the situation in the stochastic Lotka–Volterra model [33, 34] but in stark contrast with the conserved spatially extended RPS model [28]. The finite width of the frequency peak in the Fourier plot indicates that the population oscillations will decay and ultimately cease after a finite relaxation time, consistent with the damped density fluctuations visible in Fig. 2a. Therefore, in the coexistence phase, the system’s dynamics is consistent with the mean-field description, a feature that is however caused by the important influence of the particles’ spatial mobility: With relatively low but still effective (average) mobility rates (on average  $\epsilon = D = 5$ ), the dynamics of the system is dominated by local interactions (reproduction and predation) along

the boundaries of local spiral clusters. Thereby, the coexistence state is maintained for a very long time and simultaneously effective mobility mixes the system well, resulting in a remarkably faithful description of the system through the mean-field approximation. Furthermore, the (quasi)-stationary auto- and cross-correlation functions in Figs. 2c and 2d decrease from their extremal values at vanishing distance to zero within about  $\ell = 20$  lattice sites.

More importantly, Fig. 2 shows the influence of spatial disorder on the physical quantities in the May–Leonard system. We find that quenched randomness in the rates does not noticeably affect the temporal evolution of the population densities, the associated Fourier transform signals, or the decay lengths of the auto- and cross-correlation functions, irrespective of which rate is taken as random variable. This result demonstrates that our previous observation in the four-state RPS model with conservation law, where we found spatial disorder to have only minor effects, is also valid for the three-species May–Leonard system. Therefore, we conclude that predator–prey systems with cyclic competition appear to be generically robust against random spatial variations in the predation, proliferation, or mobility rates.

As demonstrated in Fig. 3, the formation of cluster patterns (see the third row of Fig. 1) ultimately renders the various observables qualitatively similar to those systems in which particles can move only via exchange processes. However, in Fig. 3 we also observe that the spatially averaged (quasi)-stationary density  $a^*$  and the peak in the Fourier transform  $|a(f)|$  vary according to the degree to which nearest-neighbor hopping is included in the model. In particular, when particle dispersal happens solely through hopping processes (4), the asymptotic species densities are relatively low, see Fig. 3a with  $\epsilon = 0$ ,  $D = 5$ ; compare with the two plots for other rate choices, and the corresponding snapshots 1b, 1g, and 1h. We attribute this lower overall species fitness to the previously noted emergence of sizeable clusters of just empty lattice sites in the absence of pair exchange processes (3), visible as small black patches in Figs. 1g and 1i. In fact, these voids effectively buffer the three species against the predation reactions (1), but also diminish the total area that can be saturated by either population, which results in an overall density reduction in the (quasi)-steady state. In contrast, when particle pair exchange processes are included, the influence of empty-site clusters is diminished and consequently the (quasi)-stationary population densities enhanced (see Fig. 3a for  $\epsilon \neq 0$ ). Furthermore, we observe that the characteristic density Fourier peak frequencies in systems where nearest-neighbor hopping is allowed are renormalized to even lower values than in runs with just pair exchange processes, which tend to better mix the system, see Fig. 3b (compare the characteristic frequency for the runs with  $D = 5$  to those with  $D = 0$ ). In Figs. 3c and 3d, we observe the presence of low-amplitude population (damped) oscillations during the decay of the correlation function, which originate from the spiral structures displayed by the system in the coexistence state (under “efficient” mobility rates) [17]. In the insets of Figs. 3c and 3d,

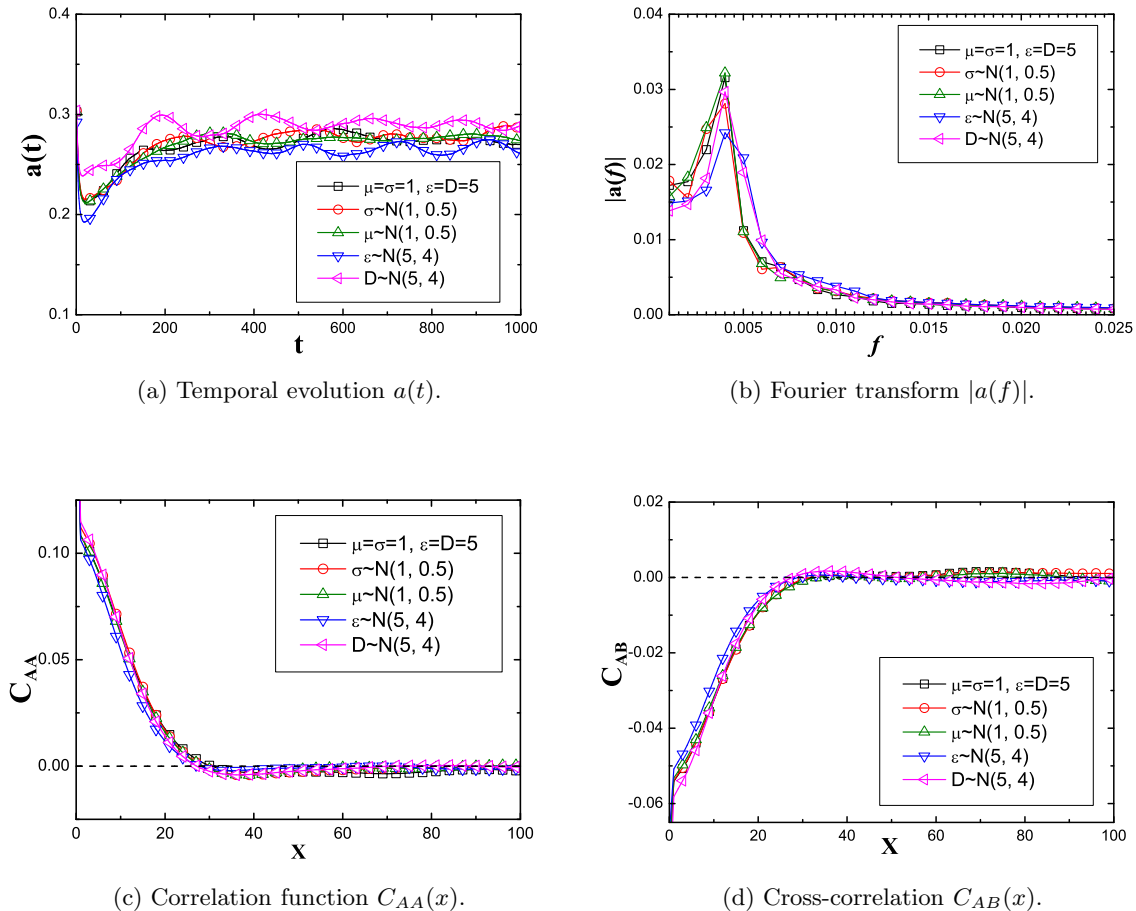


Fig. 2: (*Color online.*) Quantitative observables for a stochastic May–Leonard system with  $N = 256 \times 256$  sites, starting with equal initial densities  $a(0) = b(0) = c(0) = 1/3$  and in the presence of spatial disorder, averaged over 50 simulation runs. If unspecified, the default rate values  $\mu = \sigma = 1$ ,  $\epsilon = D = 5$  were used. The correlation functions in (c) and (d) were measured at  $t = 1000$  MCS.

we notice that the correlation functions of the model variants with only hopping processes ( $\epsilon = 0$ ) decay to zero in a less oscillatory manner than the correlation functions for the variants that include particle exchange ( $\epsilon \neq 0$ ). This is a consequence of the observed absence of well-defined spiral structures (see Figs. 1g and 1i) when the pair-exchange rate is too low to efficiently stir the system.

In summary, the pair-exchange processes suppress the presence of empty-site clusters, and despite rendering the spiral structures more diffuse (i.e., more “entangled”), they have an overall stabilizing effect on emerging spatial patterns, and consequently promote the fitness and coexistence of all three subpopulations  $A$ ,  $B$  and  $C$ .

### 3.3 Mean extinction times and their distribution

As we have discussed above, the system is efficiently stirred when the pair exchange rate  $\epsilon$  is high enough (independent

of the actual value of  $D$ ). In this case, the system is characterized by a long-lived coexistence state. However, when the pair exchange rate is below some critical value, it has been shown that the system settles in an absorbing state after an observable amount of time [15]. We here revisit and extend the analysis of such a scenario that holds true for any values of  $\epsilon$  or  $D$  by computing the mean extinction time (MET) and the distribution of extinction times. Here, for the sake of simplicity (and without loss of generality) we assume that  $\epsilon = D$  and the mobility rate therefore is  $M = 2\epsilon/N$ . In this setting, our May–Leonard model coincides with the variant considered in Refs. [15, 16, 17], where it was shown that the critical mobility threshold is  $M_c \approx 4.5 \times 10^{-4}$  (when  $\mu = \sigma = 1$ ). Indeed, when the effective mobility rate  $M$  approaches  $M_c$  from below, there is a cross-over from a coexistence (quasi-)steady state to an absorbing state.

The MET has been computed as the time when the first of the three species dies out. Figure 4 illustrates how

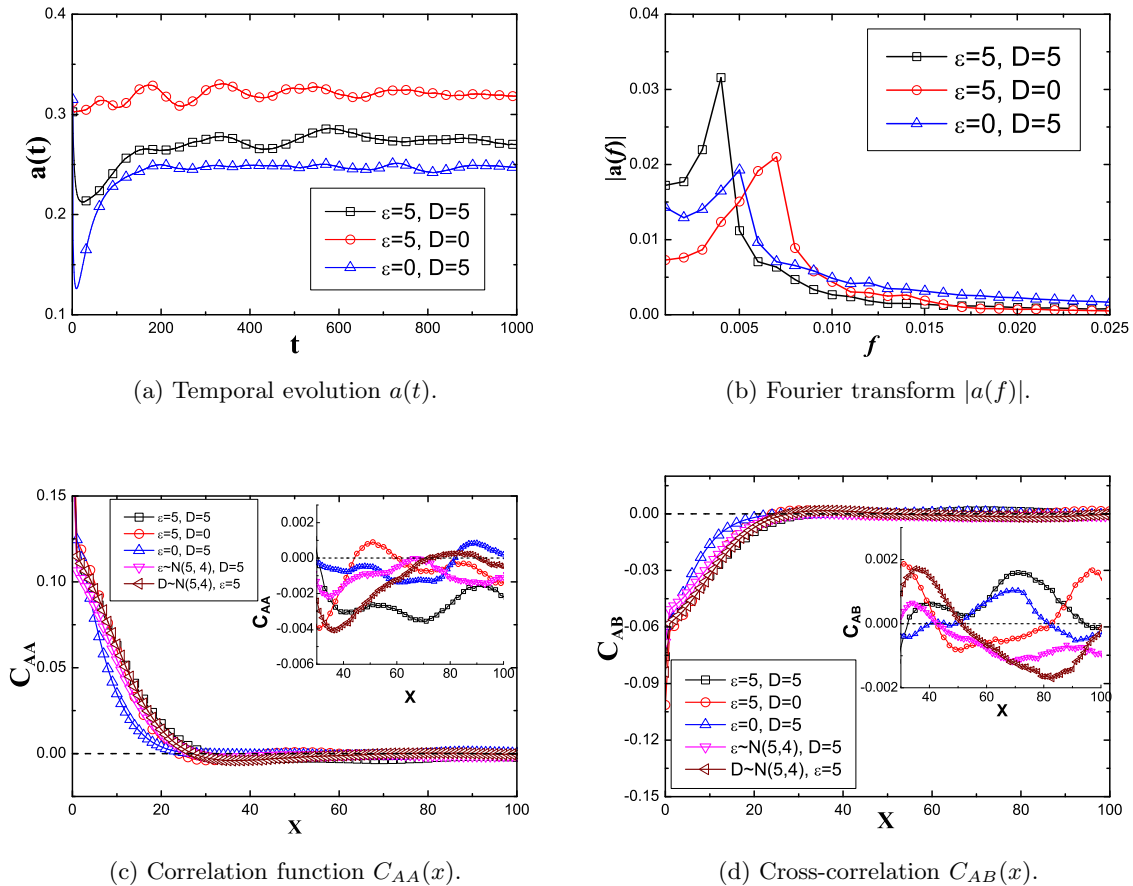


Fig. 3: (*Color online.*) Quantitative observables for a stochastic May–Leonard system with  $N = 256 \times 256$  sites, reaction rates  $\mu = \sigma = 1$ , and starting with equal initial densities  $a(0) = b(0) = c(0) = 1/3$ , with different combinations of nearest-neighbor particle exchange and hopping processes, averaged over 50 simulation runs. The correlation functions in (c) and (d) were measured at  $t = 1000$  MCS.

this MET exhibits markedly different behavior when the effective mobility rate  $M = 2\epsilon/N$  is swept through  $M_c$ . As shown in Fig. 4b, when the mobility is relatively weak ( $M = 10^{-6}$ ), the MET increases with the system size approximately according to the (zero-dimensional) functional form  $\bar{T}_{\text{ex}}(N) \sim e^{cN}/N$  (where  $c$  is a constant) [35], especially for comparatively large values  $N \sim 200 \dots 600$ . (For smaller systems with  $N < 200$ , the data do not fit this functional dependence very well, but may also not be as statistically reliable.) Yet the curvature of the graphs in Fig. 4a decreases upon raising the effective mobility, and the functional dependence on system size becomes replaced with a linear form  $\bar{T}_{\text{ex}}(N) \sim N$  for  $M > M_c$ . That is, when the mobility rate is low, the system is dominated by local interactions and species extinction is a rare event driven by a large fluctuation after an enormous amount of time. In this case, the coexistence of the three species corresponds to a metastable state. Interestingly, Fig. 4c shows that spatial disorder in the mobility rate  $M$  does not qualitatively affect the behavior of the MET: this very same

scenario applies even when  $M$  is randomly distributed. This observation further supports the conclusion that spatial variability in the mobility rates has little effect on the dynamical evolution of the system.

When the mobility rate increases and exceeds the threshold, the system is regularly driven towards extinction and biodiversity is lost, just as predicted by the zero-dimensional formulation of the model. Furthermore, the histograms of extinction times plotted in Figs. 4d and 4e show that the extinction time distributions (obtained for small systems with  $N = 20 \times 20$  sites) correspondingly evolve gradually from an approximately exponential (or Poisson) shape, albeit with fat tails, towards a (roughly) Gaussian distribution centered at  $\bar{T}_{\text{ex}}$ . In addition, the distributions remain unchanged even if spatial disorder is incorporated in the model (see the insets of Figs. 4d and 4e). The approximate quasi-exponential (or quasi-Poisson) distribution of Fig. 4d is a characteristic feature of systems where extreme events occur only after a very long time, and which are hence driven by large rare fluctuations [36]. Here, the rare

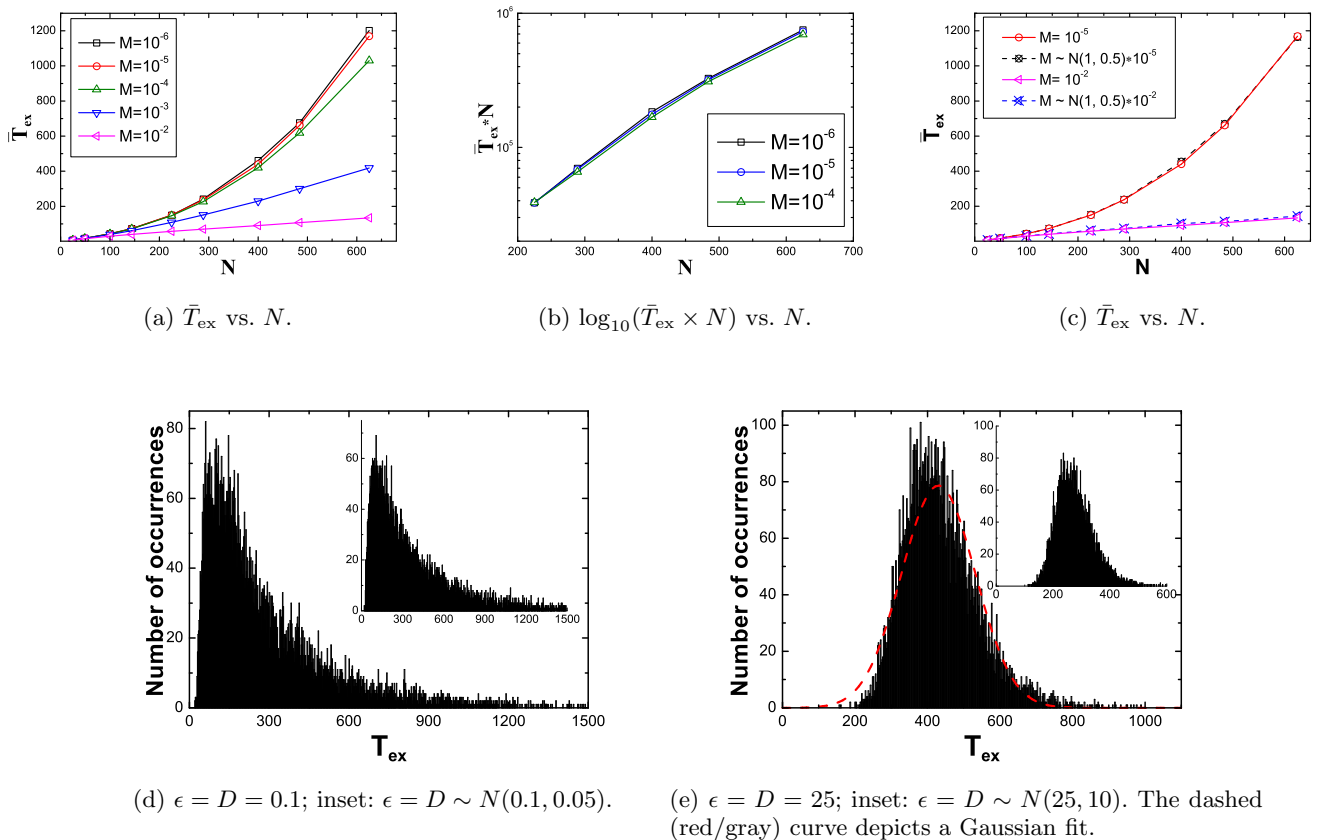


Fig. 4: (*Color online.*) (a), (b), (c) Mean extinction time (MET)  $\bar{T}_{\text{ex}}$  as function of lattice size  $N$ , for different values of the effective mobility  $M = 2\epsilon/N$  (here,  $\epsilon = D$ ), obtained from averages over 10000 Monte Carlo runs, starting with equal initial densities  $a(0) = b(0) = c(0) = 1/3$ , and reaction rates  $\mu = \sigma = 1$ . The lattice sizes are  $N = 5 \times 5$ ,  $7 \times 7$ ,  $10 \times 10$ ,  $12 \times 12$ ,  $15 \times 15$ ,  $17 \times 17$ ,  $20 \times 20$ ,  $22 \times 22$ ,  $25 \times 25$  sites. (d) and (e): Histogram of extinction times estimated from 10000 Monte Carlo runs, based on a system with lattice size  $N = 20 \times 20$ . The insets correspond to the histograms obtained for random mobility rates:  $\epsilon = D \sim N(0.1, 0.05)$  in (d) and  $\epsilon = D \sim N(25, 10)$  in (e).

extreme event is extinction of species that were previously coexisting in a metastable state for a long time period. On the other hand, the approximately Gaussian distribution of Fig. 4e is typical of systems where random fluctuations are of weak intensity [37]. In our competing three-species system, it is associated with the absorbing state that corresponds to species extinction happening within an “observable” time range, as in the zero-dimensional counterpart of the model [15, 16, 17]. These numerical observations support the method suggested in Ref. [15] for identifying the nature of (quasi-)steady states in the simulation of RPS models: A reasonable criterion is that the system remains at the steady state if three species still coexist after simulation time  $t \sim N$ , otherwise, the system evolves to an absorbing state.

## 4 Conclusion

In this paper, we have demonstrated that quenched spatial disorder in either the reaction or the mobility rates does not significantly affect the temporal evolution, Fourier signals, spatial correlation functions, or mean extinction times in stochastic spatial May–Leonard models (i.e., four-state RPS models without total particle number conservation) in two dimensions. In combination with our previous results for conserved three-species RPS systems [28], we conclude that such cyclic predator-prey systems appear to be generically robust against spatial variability of the rates. Here, the randomized reaction rates remain attached to the lattice sites, mimicking environmental variations that do not change over time. As there exist a number of systems, e.g. in ecology [12] and microbiology [14], where the competition among species is cyclic, an important implication of our findings is that the environmental variability of the parameters can essentially be neglected in the mathematical description of those systems. In addi-



tion, through removing the hopping process by letting  $D = 0$ , we observe that particle pair exchange processes promote the formation of sharp spiral patterns. In our spatial stochastic system, we measure the population oscillation frequency to be much lower than predicted by the mean-field rate equations, similar to the situation in two-species Lotka–Volterra models [33,34], but in stark contrast with our numerical results for conserved RPS model variants [28]. This downward frequency renormalization is enhanced by the presence of nearest-neighbor hopping processes. Moreover, we find a remarkable gradual transformation in the dependence of the mean extinction time on system size, and the shape of the associated extinction time distribution, when the effective mobility rate crosses the critical threshold separating the coexistence from the absorbing state: When the mobility rate is low, the distribution of extinction times is approximately exponential, and species coexistence corresponds to a long-lived metastable state. In this case extinction is driven by large, rare fluctuations and the mean extinction time essentially grows exponentially with the population size. Above the critical mobility threshold, the extinction times are approximately distributed according to a Gaussian. In this situation, the noise is of weak intensity and the mean extinction time grows linearly with the population size. Interestingly, we find that these results remain valid for both non-random as well as for randomly distributed mobility rates.

This work is in part supported by Virginia Tech’s Institute for Critical Technology and Applied Science (ICTAS) through a Doctoral Scholarship. We gratefully acknowledge inspiring discussions with George Daquila, Uli Dobramysl, Michel Pleimling, Matt Raum, and Royce Zia.

## References

1. J. Maynard Smith, *Evolution and the Theory of Games* (Cambridge University Press, Cambridge, U.K., 1982)
2. J. Hofbauer and K. Sigmund, 1998 *Evolutionary games and population dynamics* (Cambridge University Press, Cambridge, U.K., 1998)
3. M. A. Nowak, *Evolutionary Dynamics* (Belknap Press, Cambridge, USA, 2006)
4. G. Szabó, *Phys. Rep.* **446**, 97 (2007)
5. R. M. May and W. J. Leonard, *SIAM J. Appl. Math.* **29**, 243-253 (1975)
6. R. M. May, *Stability and Complexity in Model Ecosystems* (Cambridge University Press, Cambridge, U.K., 1974)
7. J. Maynard Smith, *Models in Ecology* (Cambridge University Press, Cambridge, U.K., 1974)
8. R. E. Michod, *Darwinian Dynamics* (Princeton University Press, Princeton, USA, 2000)
9. R. V. Sole and J. Bascompte, *Self-Organization in Complex Ecosystems* (Princeton University Press, Princeton, USA, 2006)
10. D. Neal, *Introduction to Population Biology* (Cambridge University Press, Cambridge, U.K., 2004)
11. L. Frachebourg and P. L. Krapivsky, *J. Phys. A: Math. Gen.* **31**, L287 (1998)
12. B. Sinervo and C. M. Lively, *Nature (London)* **380**, 240 (1996)
13. K. R. Zamudio and B. Sinervo, *Proc. Natl. Acad. Sci. (USA)* **97**, 14427 (2000)
14. B. Kerr, M. A. Riley, M. W. Feldman and B. J. M. Bohannan, *Nature (London)* **418**, 171 (2002)
15. T. Reichenbach, M. Mobilia and E. Frey, *Nature (London)* **448**, 1046 (2007)
16. T. Reichenbach, M. Mobilia and E. Frey, *Phys. Rev. Lett.* **99**, 238105 (2007)
17. T. Reichenbach, M. Mobilia and E. Frey, *J. Theor. Biol.* **254**, 368 (2008)
18. T. Reichenbach, M. Mobilia and E. Frey, *Banach Center Publications* Vol. **80**, 259 (2008)
19. M. Peltomäki and M. Alava, *Phys. Rev. E* **78**, 031906 (2008)
20. T. Reichenbach, M. Mobilia and E. Frey, *Phys. Rev. E* **74**, 051907 (2006)
21. M. Berr, T. Reichenbach, M. Schottenloer and E. Frey, *Phys. Rev. Lett.* **102**, 048102 (2009)
22. L. Frachebourg, P. L. Krapivsky and E. Ben-Naim, *Phys. Rev. E* **54**, 6186 (1996)
23. A. Provata, G. Nicolis and F. Baras, *J. Chem. Phys.* **110**, 8361 (1999)
24. K. I. Tainaka, *Phys. Rev. E* **50**, 3401 (1994)
25. G. Szabó and A. Szolnoki, *Phys. Rev. E* **65**, 036115 (2002)
26. M. Perc, A. Szolnoki and G. Szabó, *Phys. Rev. E* **75**, 052102 (2007)
27. G. A. Tsekouras and A. Provata, *Phys. Rev. E* **65**, 016204 (2001)
28. Q. He, M. Mobilia and U. C. Täuber, *Phys. Rev. E* **82**, 051909 (2010)
29. G. Szabó, A. Szolnoki and R. Izsák, *J. Phys. A: Math. Gen.* **37**, 2599 (2004)
30. A. Szolnoki and G. Szabó, *Phys. Rev. E* **70**, 037102 (2004)
31. J. C. Claussen and A. Traulsen, *Phys. Rev. Lett.* **100**, 058104 (2008)
32. U. Dobramysl and U. C. Täuber, *Phys. Rev. Lett.* **101**, 258102 (2008)
33. M. Mobilia, I. T. Georgiev and U. C. Täuber, *J. Stat. Phys.* **128**, 447 (2007)
34. M. J. Washenberger, M. Mobilia and U. C. Täuber, *J. Phys.: Condens. Matter* **19**, 065139 (2007)
35. M. Mobilia, *J. Theor. Biol.* **264**, 1 (2010)
36. H. Touchette, *Phys. Rep.* **478**, 1 (2009)
37. C. W. Gardiner, *Handbook of Stochastic Methods* (Springer-Verlag, Berlin, 2nd ed., 2002)